water

Article

Impact of Land Use Change on the Water Environment of a Key Marsh Area in Vientiane Capital, Laos

Keophouxone Phanmala, Yizhe Lai and Kang Xiao *

Beijing Yanshan Earth Critical Zone National Research Station, College of Resources and Environment, University of Chinese Academy of Sciences, Beijing 101408, China; keophouxone@gmail.com (K.P.); laiyizhe21@mails.ucas.ac.cn (Y.L.)
* Correspondence: kxiao@ucas.ac.cn

Abstract: The water environment is critical to maintaining ecosystem balance and human well-being globally. It is essential to comprehend the effects of land use change on water quantity and quality for sustainable development of the urban environment. Expansion of urban areas leads to intensified human activity and increased pollution loads in natural waterbodies. This study aimed to monitor changes in land use over a span of two decades to evaluate the condition of the water environment in That Luang Marsh (TLM). The land use and land cover (LULC) classes, including agricultural land, bare land, built-up land, vegetation, waterbody, and wetland, were categorized via Landsat images utilizing the maximum likelihood algorithm. A digital elevation model was used to estimate the water surface area and volume, and the nutrient delivery ratio model was employed to analyze nutrient distribution across the LULC classes. The results showed that from 2001 to 2020, the bare land, built-up, waterbody, and wetland areas increased by 29.92, 18.64, 0.87, and 0.16 times, respectively, while the agricultural and vegetation land decreased by 0.80 and 0.76 times, respectively. A binary logistic regression model for influential factors implies that road network expansion within the special economic zone in TLM could result in an increase in residential areas, thereby impacting the LULC classes. The increase in water volume showed a robust correlation with the expansion of built-up land, bare land, and waterbody. TLM had an average nitrate-nitrogen export of 317 tons/year with a 95% confidence interval of (56, 770) tons/year in 2020. The distribution over LULC classes affected the export, which varied dynamically. Vegetation land had the highest nitrate-nitrogen load of 0.57 tons/ha/year, probably due to poorly managed use of fertilizers. The developed land surface for an artificial lake could lead to an increase in the water volume, which could be involved in the dilution of nutrient concentration. Therefore, it is crucial to prioritize policies that aim to establish sustainable urban water environments through rational urban planning and by making LULC management a primary consideration, especially for developing countries undergoing similar processes of urbanization along the Mekong River in Southeast Asia.

Keywords: That Luang Marsh; land use and land cover (LULC); water availability; nitrate-nitrogen export

Citation: Phanmala, K.; Lai, Y.; Xiao, K. Impact of Land Use Change on the Water Environment of a Key Marsh Area in Vientiane Capital, Laos. *Water* **2023**, *15*, 4302. https://doi.org/10.3390/w15244302

Academic Editor: Christos S. Akratos

Received: 6 November 2023
Revised: 11 December 2023
Accepted: 14 December 2023
Published: 18 December 2023

1. Introduction

Increasing population size and changes in land use create pressure on urban marshland ecosystems [1]. In order to effectively plan for conservation and management, it is necessary to understand the natural conditions of marsh systems, particularly in terms of hydrology, water quality, and aspects of the ecosystem [2]. Urban marshland slows down the water flow and retains pollutants including nutrients and toxic chemicals discharged from urban areas [3,4]. These marshlands also play a critical role in mitigating the risk of urban flooding, serve as a vital source of food [5] (EPA, 2016), and are crucial components in developing sustainable nature-based solutions [6] (Ferreira et al., 2023).

Changes in land use and land cover (LULC) of marsh areas are crucial factors in modifying the capacity of marsh ecosystems to provide essential services [7,8]. These changes have a particularly significant impact on soil erosion and runoff, which result in the export of pollutants such as nutrients and sediment into watercourses [2,9]. The expansion of agricultural land and urban areas leads to an increase in nutrient loads due to surface and stormwater runoff into waterbodies [10,11], which results in significant eutrophication. In addition, climate conditions control the change in water quantity at the watershed scale [9], whereby land cover change affects climate parameters influenced by human activities. In the case of urban marshland, the discharge could be relatively high even in the dry season because of the discharge from urban areas.

Water quality and quantity are crucial for improving environmental flow, sustainable agriculture, and human health [12,13]. Many global studies have investigated the correlation between LULC and water quantity/quality in various regions. In the Songkhram River Basin, Thailand, a regulated land use change resulted in a 1.05% (from 5.3% to 6.35%) increase in streamflow [14], whereas LULC change in a tropical catchment in Tanzania showed a decrease in flow of 6–8% in 2030 [15]. The Nyazvidzi catchment in Zimbabwe showed a weak correlation between land use and runoff [16]. In Huang-Huai-Hai Plain, China, LULC change had negative effects on water environment quality [17]. Urbanization seriously reduced water quality and quantity in India [18,19]. LULC changes need to be monitored to ensure a sustainable environment as urban areas have been shown to significantly contribute to nutrient export [20–22]. Farming and populated areas have been found to cause water pollution [2,9,23–26], whereas forested areas exhibit a weak correlation [27,28]. These impacts are a concern in Laos, particularly in That Luang Marsh (TLM) in the capital, Vientiane (see Figure 1).

In recent years, the Vientiane area, particularly TLM, has undergone rapid development. In 2011, a special economic zone with complex infrastructures was developed downstream of TLM, with the effects of LULC. The opening of the "China-Laos Railway" in December 2021 further accelerated the development of TLM. Little attention has been given to the impacts of LULC on water quality and quantity in this marsh area, and LULC is not frequently monitored even for Vientiane as a whole. From 2016 to 2020, urbanization caused a decrease in the amount of farmland in Vientiane [29], whereas from 1995 to 2018, the amount of waterbody area gradually increased [30]. These studies are vital for sustainable urban planning in terms of LULC change. In general, the maximum water stock of TLM was recorded in December, while the lowest was recorded in April [31]. Some studies indicated that urban areas released a high amount of nutrients into TLM during the dry season [32,33], and decentralized wastewater treatment was therefore recommended [34]. These issues are critical in the planning of different aspects of water environmental management such as urban wastewater treatment, irrigation schemes, and ecosystem balance within Vientiane. However, investigations into the correlation between LULC and water quality/quantity are relatively lacking. Therefore, it is imperative to clarify the impact of LULC change on water quality and quantity to establish comprehensive and sustainable urban development planning, which is especially significant for developing countries in the process of urbanization.

This study examined how changes in land use impact water quantity and quality in the key urban marshland of TLM in Vientiane. The results could assist in the development of policy measures to minimize the effect of LULC change on the water environment in the future. The objectives of this study are to (i) analyze the changes in LULC over the course of two decades, (ii) estimate the surface water quantity affected by LULC change, and (iii) evaluate the nitrate-nitrogen distribution in LULC classes relevant to marsh areas. Figure 2 shows the framework of this study.

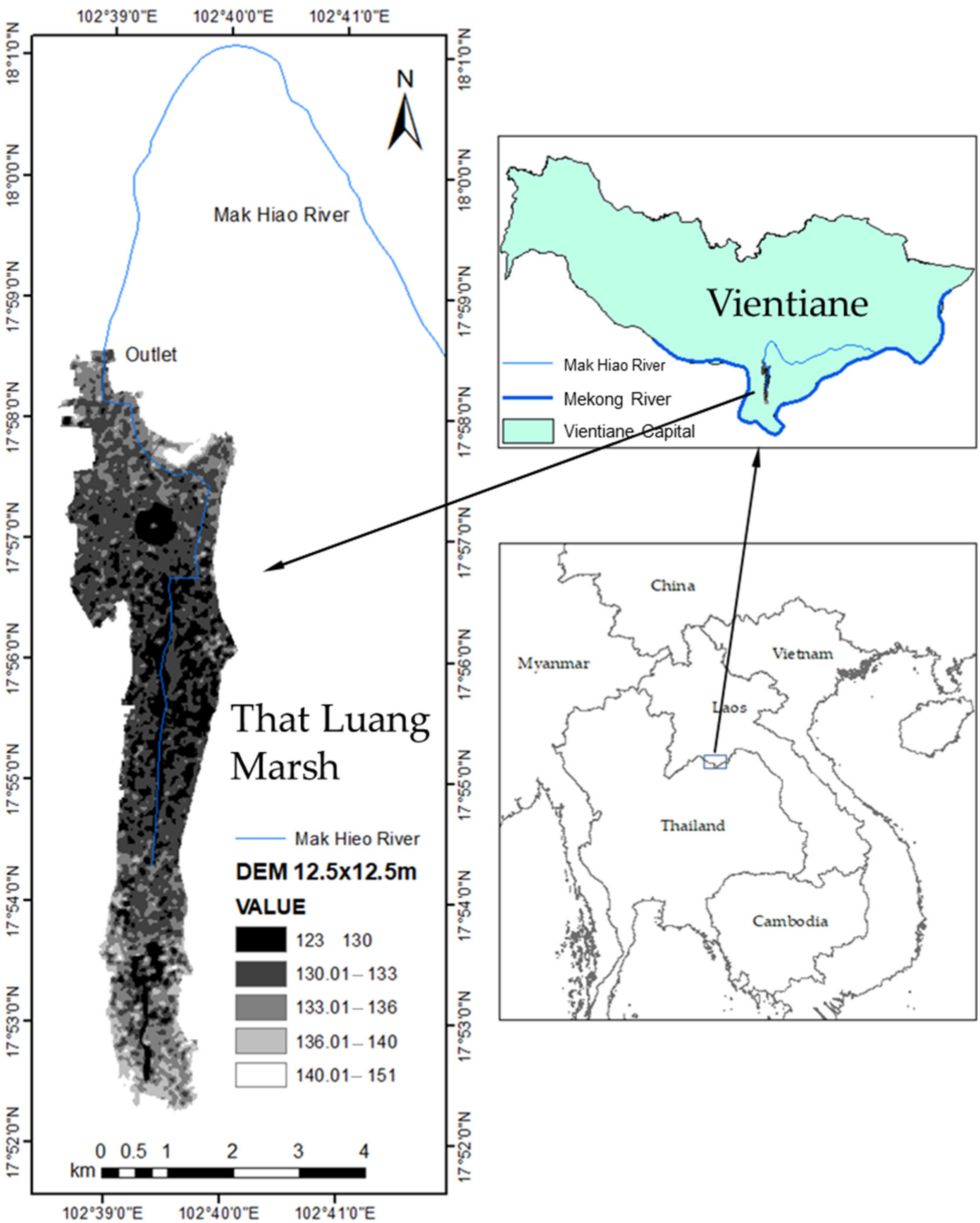

Figure 1. Location of the study area.

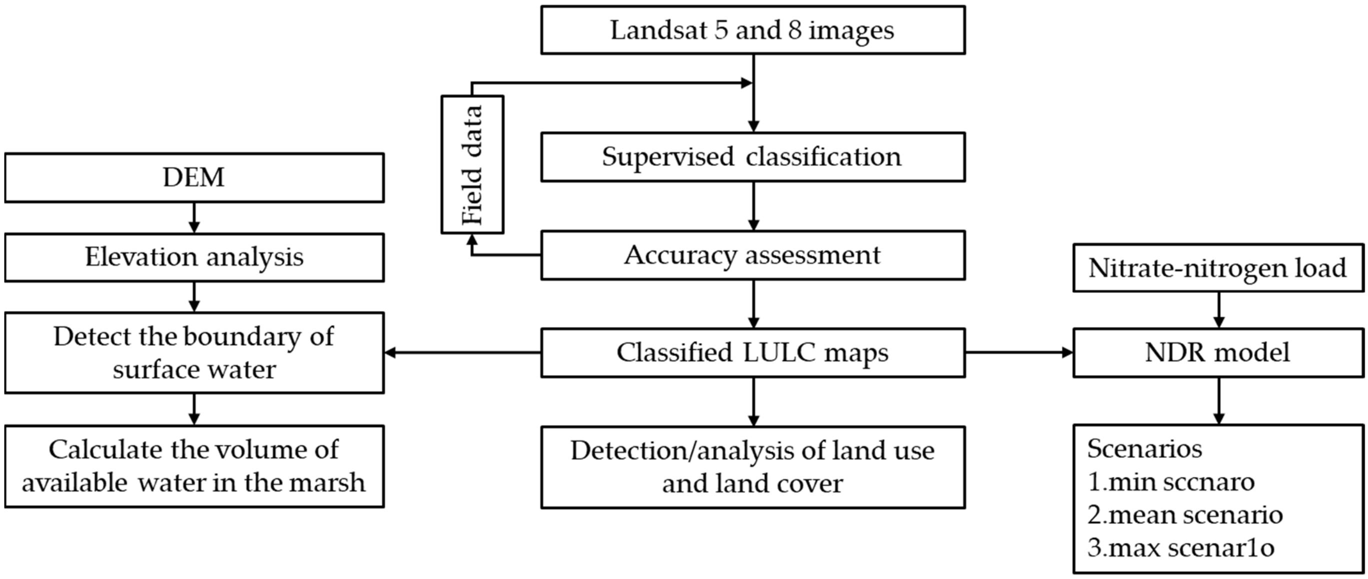

Figure 2. Research framework.

2. Materials and Methods

2.1. Study Area

TLM, located on the eastern edge of Vientiane [35], is the largest wetland in the area, with coordinates of 17°56′ N and 102°39′ E (Figure 1). The wetland elevation ranges from 123 to 151 m above the mean sea level. Based on recorded data (1970–2009) from the Department of Meteorology and Hydrology of Laos, the annual average temperature ranged from 22.2 to 29.5 °C, and the average annual rainfall was 1664 mm. This area has two distinct seasons, the dry season from May to October and the rainy season from November to April, due to its tropical monsoon climate. There are 17 villages in the vicinity of TLM [36]. Recent land surface development has resulted in barren areas dominating TLM's land area, which has also seen an expansion of built-up areas into the marsh area. Recently, a human-made channel, the Mak Hiao River, has been constructed to connect the upstream marsh to the main drainage river. The river receives drained water from urban areas and TLM through natural riverine wetland before entering the Mekong River.

2.2. Data Collection and Preparation

The input data for analysis included remote sensing, GIS data, and other relevant data, as shown in Table 1. The baseline year 2001 was selected because Laos has been listed among the fastest-growing economies in the world since 2000 according to the World Bank's report on the Lao PDR Country Economic Memorandum. Since 2000, the government of Lao PDR has promoted domestic and foreign investment, triggering significant changes in LULC.

Table 1. Data collection and sources.

Data	Data Acquisition	Source
Remote sensing	Landsat 5 TM, 27 March 2001 (C2L2)	USGS
	Landsat 5 TM, 06 March 2005 (C2L2)	USGS
	Landsat 5 TM, 20 March 2010 (C2L2)	USGS
	Landsat 8 OLI-TIRS, 18 March 2015 (C2L2)	USGS
	Landsat 8 OLI-TIRS, 31 March 2020 (C2L2)	USGS
GIS data	DEM 2000 and DEM 2014	Google Earth, ALOS PALSAR
	Road network	https://www.openstreetmap.org/ (accessed on 20 October 2022)

Table 1. *Cont.*

Data	Data Acquisition	Source
GIS data	Stream network	https://www.openstreetmap.org/ (accessed on 20 October 2022)
	Commercial food services	Field survey
	Degree of slope	Generated from DEM
Secondary data	Average yearly rainfall between 1975 and 2014	LSB [37]
	Monthly streamflow between 2009 and 2010	JICA [32]
	Monthly nitrate-nitrogen between 2009 and 2010	JICA [32]
	Nitrate-nitrogen retention coefficients	InVEST user guideline

Note: LSB: Lao Statistics Bureau.

2.3. Classification of Land Use and Land Cover (LULC) Classes

A supervised classification methodology was applied with ArcMap 10.7 to satellite images captured in 2001, 2005, 2010, 2015, and 2020. This method has been extensively employed in LULC classification utilizing the maximum likelihood algorithm [38–40]. The maximum likelihood classification method nested in the ArcMap 10.7 software was utilized for the LULC classification. As a supervised classification method, the maximum likelihood classification can effectively evaluate similarity through the mean and variance of samples. It is widely used for multi-class feature recognition with the help of high-resolution maps (e.g., Google Earth maps) for the training samples. In total, 600 training samples were collected to classify the LULC for a single year in the study area. The output raster of the maximum likelihood method was converted to vector data. Then, the vector data were manually checked and digitized using high-resolution maps such as Google Earth Pro maps to identify the actual boundaries, especially for waterbodies and wetlands, which enabled the definition of real visible images from different years [30,41]. After successful interpretation of the supervised classification, the LULC was categorized into six classes, as described in Table 2: agricultural land, bare land, built-up land, vegetation, waterbody, and wetland.

Table 2. Definition of land use and land cover (LULC) classes.

LULC Class	Description
Agricultural land	Land for cultivation, including rice paddies, and garden land
Bare land	Empty land, clearing land surfaces, and active excavations
Built-up land	Construction land, including land for industries, factories, residences, buildings, houses, roads, etc.
Vegetation	Degraded forests, shrubs, fruit trees, rubber trees, and other forms of vegetation higher than 2 m
Waterbody	Open water surfaces, fish ponds, and drainage canals
Wetland	Marshlands that are covered by water and grass

The confusion matrix method was used to evaluate the level of accuracy of the LULC classification in order to clarify the relationship between raw (satellite) images and their classified versions [39,42,43]. Randomized raster values were extracted from the reference image (Landsat image) for each classified image taken in 2001, 2005, 2010, 2015, and 2020, using a total of 360 reference points (60 points for each LULC class). These values were then imported into the classified images for comparison. The classification accuracy was confirmed using ground truth data and Google Earth Pro maps. A confusion matrix was utilized to evaluate the agreement between the classification and ground data, utilizing Kappa statistics to measure the accuracy of both the producer and the user (Equation (1) to Equation (4)) [44]. Each element (x_{kj}) in the confusion matrix represents the number of samples of real land use class k that were classified as class j, so that x_{kk} represents the number of correctly classified samples. Table 3 summarizes the accuracy of the LULC classification for the five years.

$$\text{Producer's accuracy}(\%) = \left(\frac{x_{kk}}{x_{k+}}\right) \times 100 \quad (1)$$

$$\text{User's accuracy}(\%) = \left(\frac{x_{kk}}{x_{+k}}\right) \times 100 \quad (2)$$

$$\text{Overall accuracy} = \frac{1}{N}\sum_{k=1}^{r} x_{kk} \quad (3)$$

$$\text{Kappa coefficient} = \frac{N\sum_{k=1}^{r} x_{kk} - \sum_{k=1}^{r}(x_{k+}.x_{+k})}{N^2 - \sum_{k=1}^{r}(x_{k+}.x_{+k})} \quad (4)$$

where r is the class number (r = 6 for this study), N is the number of total pixels, x_{k+} represents the sum of values in row k, and x_{+k} represents the sum of values in column k. The Kappa coefficient values of 0–0.2, 0.2–0.4, 0.4–0.6, 0.6–0.8, and 0.8–1 represent slight, fair, moderate, substantial, and almost perfect agreement, respectively [44].

Table 3. Accuracy of LULC classification.

LULC Class	2001		2005		2010		2015		2020	
	PA	UA	PA	UA	PA	UA	PA	UA	PA	UA
Agricultural land (%)	75.8	83.3	90.0	90.0	82.1	76.7	90.0	90.0	81.8	90.0
Bare land (%)	86.2	83.3	96.7	96.7	96.4	90.0	87.5	93.3	88.9	80.0
Built-up land (%)	90.0	90.0	96.7	96.7	90.9	98.0	93.1	90.0	81.8	90.0
Vegetation (%)	83.3	83.3	88.2	100.0	92.9	86.7	85.3	96.7	100.0	100.0
Waterbody (%)	100.0	93.3	100.0	96.7	100.0	100.0	100.0	100.0	90.9	100.0
Wetland (%)	86.7	86.7	92.6	83.3	78.8	86.7	100.0	83.3	87.5	70.0
OA (%)	86.7		93.9		90.0		92.2		88.3	
KC	0.84		0.93		0.88		0.91		0.86	

Note: PA = producer accuracy; UA = user accuracy; OA = overall accuracy; KC = Kappa coefficient.

2.4. Characterization of LULC Change

The classified maps were utilized to calculate and analyze the change pattern in the TLM area during 2001–2005, 2005–2010, 2010–2015, and 2015–2020. The Geoprocessing tool in ArcMap was used to visualize the changes in the area of each LULC class and the class-to-class transitions for each five-year period. For each LULC class, the rate of change across any time period was calculated as follows [43,45]:

$$\text{Rateofchange} = \frac{\text{AT}_2 - \text{AT}_1}{Z} \quad (5)$$

where AT_1 and AT_2 are the specific land areas (ha) at times 1 and 2, respectively, and Z is the time interval (year).

A binary logistic regression analysis was conducted by utilizing IBM SPSS Statistics 27 to explain the relationship between LULC classes and five physical and socioeconomic factors (i.e., road network, stream, commercial food services, elevation, and degree of slope) in terms of locational preference. The attribute table of multi-raster values was imported into SPSS for the analysis. Model outputs were evaluated using the receiver operating characteristic (ROC) curve. The area under the curve (AUC) value ranged from 0 to 1, with an AUC value higher than 0.7 (or 0.5) indicating a satisfactory (or moderate) fit of the logistic regression model [46–48].

2.5. Analysis of Water Availability

The estimation of water storage was carried out by using 3-D analysis in ArcScene based on the results of LULC classification with 5-year intervals (2001–2005, 2005–2010, 2010–2015, and 2015–2020). The water volumes were calculated by combining the water-body boundaries identified in the LULC class classification and a digital elevation model (DEM). DEM 2000 was used for the years 2001, 2005, and 2010, while DEM 2014 was used for the years 2015 and 2020. The average water volume (V_{w}) was calculated as follows:

$$V_{\mathrm{w}} = A_{\mathrm{w}} \times \mathrm{WL}_{\mathrm{av}} \quad (6)$$

where A_{w} is the area of surface water from analysis of the water boundaries on the land use map and $\mathrm{WL}_{\mathrm{av}}$ is the average water level in the marsh in that year, which can be derived from

$$\mathrm{WL}_{\mathrm{av}} = \mathrm{WS}_{\mathrm{ele}} - \mathrm{ELE}_{\mathrm{av}} \quad (7)$$

where $\mathrm{WS}_{\mathrm{ele}}$ is the elevation of surface water and $\mathrm{ELE}_{\mathrm{av}}$ is the average elevation of pixels under water.

The water quality of TLM was assessed using the nutrient delivery ratio (NDR) of the InVEST model (www.naturalcapitalproject.org (accessed on 20 October 2022)), taking nitrate-nitrogen (NO_3^--N) as a representative pollutant. This model maps nutrient sources from watersheds, calculates their transport to streams, and evaluates nutrient retention based on environmental conditions on the land surface [49]. The nutrient loads represent the amount of nutrients contributed by each pixel of the land use image. Surface runoff or precipitation is a critical factor in transporting nutrients across the slope of the land surface. Parameters utilized in the NDR model were based on the NatCap database in the InVEST user guideline which provides a non-exhaustive list of local references for nutrient loads and retention efficiencies. The model calibration was performed by adjusting the parameters of retention efficiency, threshold flow accumulation, and hydrological connectivity to achieve the best consistency of calculated values with observed data. The utilization of model-provided parameters to simulate nutrient delivery was similarly applied in some other studies [50–52]. According to the available data on monthly water quality monitoring conducted by JICA [32] in 2009 and 2010 in the study area, the monitoring points were overlaid on the LULC map to identify the corresponding point for each LULC class. For instance, where there is a monitoring point at the outlet of a residential built-up area, the pollutant load at this point could represent the contribution by the built-up class. The loads of other LULC classes were estimated in a similar way. Min, mean, and max values represent the nitrate-nitrogen load in the range from the lowest to the highest, and they were used for calculating the total export in the scenarios of min, mean, and max, respectively. Regarding the limitation of available hydrological and water quality data, the bootstrap statistical method was used to resample the dataset to create a series of simulated samples for a more informative description of the data distribution, as shown in Table 4. The optimal calibration parameters, shown in Table S6, were validated by using a point of observed data at the outlet of the marsh, which was measured at 0.37 kg/ha/year [32]. For such calculations, the nitrate-nitrogen export at downstream pixels without retention is described as follows [53]:

$$\mathrm{NDR}_i = \mathrm{NDR}_{0,i}\left(1 + \exp\left(\frac{\mathrm{IC}_0 - \mathrm{IC}_i}{k}\right)\right)^{-1}. \quad (8)$$

where IC_0 and k are calibration parameters that define the shape of the NDR-IC relationship, IC_i is an index of connectivity (a topographic index representing the hydrological connectivity, i.e., how likely it is for the nutrients on a pixel to reach the stream), and $\mathrm{NDR}_{0,i}$

is the proportion of nitrate-nitrogen that is not retained by downslope pixels. The total nitrate-nitrogen export at the effluent of the marsh was then computed as follows [53]:

$$x_{\text{exp\_total}} = \sum_i x_{\text{exp\_}i} \tag{9}$$

where $x_{\text{exp\_}i}$ is the nitrate-nitrogen export from each LULC class.

Table 4. Statistics of nitrate-nitrogen load in different LULC classes.

LULC Class	Descriptive Statistics from Raw Data (kg/ha/Year)				Mean 95% Confidence Interval by Bootstrap Estimation (kg/ha/Year)		Other Parameters		
	Min	Mean	Max	Standard Deviation	Lower	Upper	Retention Efficiency	Critical Length	Proportion of Subsurface
Agricultural land	0.16	9.99	28.38	10.32	3.40	17.71	0.56	12.5	0
Bare land	0.99	14.86	40.50	14.02	5.09	25.08	0.05	12.5	0
Built-up land	30.10	281.34	1536.44	424.51	37.07	661.08	0.15	12.5	0
Vegetation	0.00	568.62	2369.51	844.68	47.33	1158.82	0.80	12.5	0
Waterbody	34.86	478.13	2574.09	693.57	107.74	1118.42	0.25	12.5	0
Wetland	18.79	415.32	2649.20	699.96	63.91	1070.62	0.85	12.5	0

Note: Raw data were adopted from JICA [32]; bootstrap method was used 1000 times for parameter estimation.

3. Results and Discussion

3.1. Characteristics of Land Use Change

The areas of various LULC classes from 2001 to 2020 are illustrated in Figure 3. The overall accuracy and Kappa statistics of the satellite-image-based classification were 87–94% and 0.84–0.93, respectively, demonstrating that the classification was acceptable (see Table 3) [38,47]. From 2001 to 2020, agricultural and vegetation lands decreased rapidly from 1121.9 ha (70.7% of the total area of TLM) and 28.7 ha (1.8%) to 226.3 ha (14.3%) and 6.9 ha (0.4%), respectively, whereas the built-up land and bare land increased rapidly from 11.4 ha (0.7%) and 18.9 ha (1.2%) to 224.3 ha (14.1%) and 583.1 ha (36.7%), respectively. This reflected the abandonment of agricultural land and the development of urban areas [29]. The most significant change occurred during 2010–2015 for agricultural, built-up, and bare land, while it was during 2015–2020 that the vegetation area decreased most significantly.

From 2001 to 2020, the waterbody area increased gradually from 105.7 ha (6.7%) to 197.2 ha (12.4%). This may be due to the encroachment of human activities from 2001 to 2020 onto the southern part of TLM, such as ponds for recreation and small fishery farming, and the construction, from 2010 to 2020, of a 350 ha circular lake in the northern region of TLM as part of the special economic zone [54]. A similar trend in the waterbody area of Vientiane was reported by Faichia et al. and Vongpraseuth [30,55]. Wetland areas are known for their significant natural purification and water storage functions. The area of wetland fluctuated over time and decreased from 2015 to 2020.

The specific changes in LULC area from one class to another during different periods are shown as transfer matrices in Figure 4. From 2001 to 2005, there was a 22.4% conversion of bare land to built-up area, while vegetation area and wetland area saw 16.2% and 8.4% changes to agricultural land, respectively. In the subsequent period, 2005–2010, only 28.1% of bare land remained, while 31.3%, 8.8%, and 10.2% of bare land, vegetation land, and waterbody, respectively, were converted to built-up areas. The wetland area experienced a 15.3% decrease while the waterbody increased by the same percentage. Agricultural land and waterbody witnessed gains of 14.7% and 9.9%, respectively. From 2010 to 2015, an increase in abandoned agricultural land was observed, with 31.7%, 19.4%, and 10.5% of area converted to bare land, wetland, and built-up area, respectively. Finally, from 2015 to 2020, deforestation of the settlement area was observed, resulting in the conversion of approximately 46.1% and 25.4% of vegetation land to built-up and bare land, respectively.

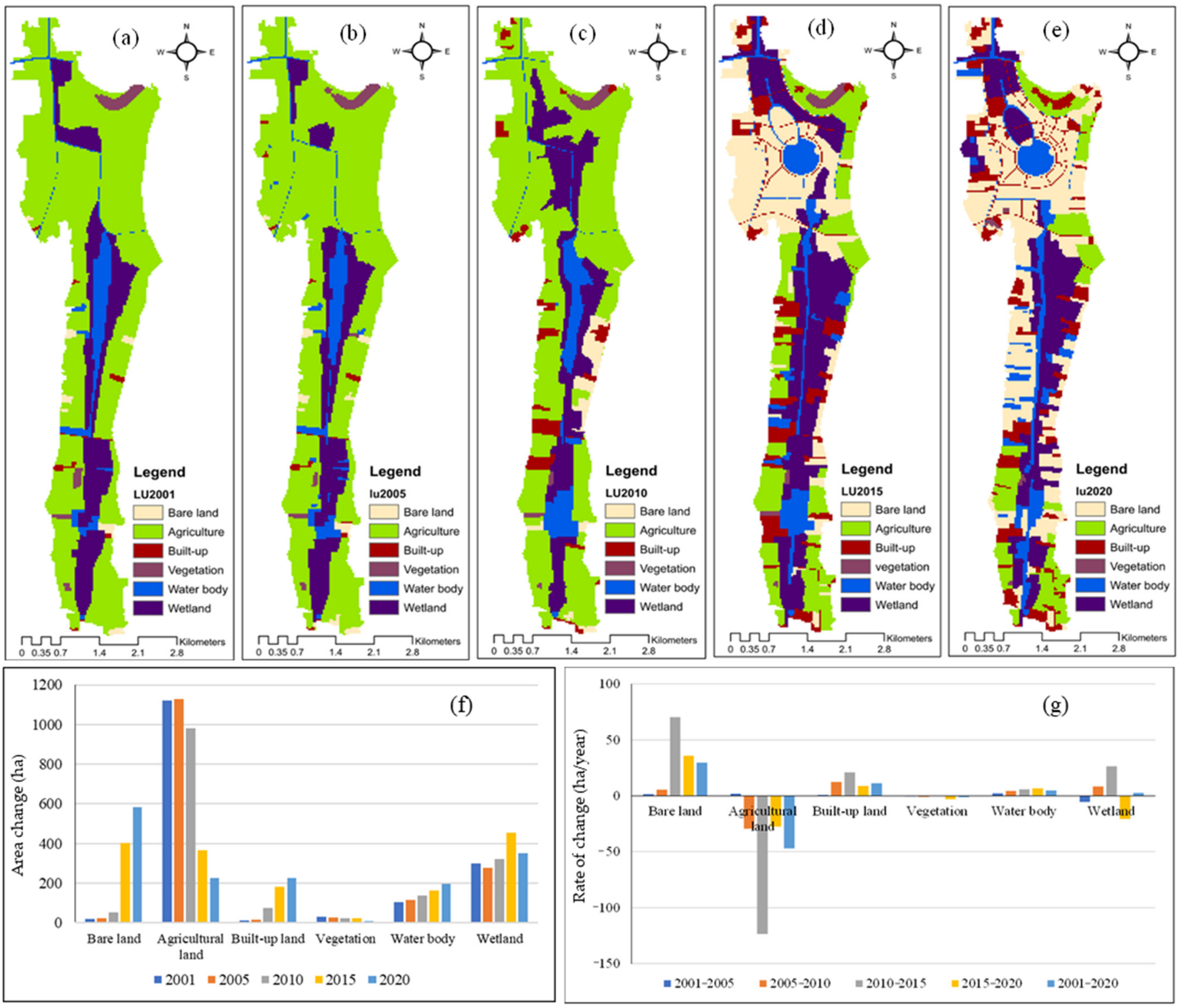

Figure 3. LULC distribution maps of (**a**) 2001, (**b**) 2005, (**c**) 2010, (**d**) 2015, and (**e**) 2020; statistics of LULC change for (**f**) area change and (**g**) rate of area change.

In terms of waterbody, there was a slight loss of 5.4% and gain of 3.0% in exchanges with wetland during 2001–2005. However, during 2005–2010, waterbody was converted to agricultural land (8.9%), built-up area (10.2%), and wetland (9.9%) but gained from wetland (15.3%) and bare land (8.3%). The following period, 2010–2015, exhibited the most significant exchanges of waterbody with wetland (17.4% gain and 38.7% loss) and built-up area (21.5% gain and 5.4% loss). Furthermore, waterbody became bare land continuously by 4.9% and 11.7% during 2010–2015 and 2015–2020, respectively. These two periods presented quite stable transitions of waterbody to built-up areas by 5.3–5.4% (Figure 4).

A binary logistic regression model was utilized to measure the correlation between the dependent variable (identification of each LULC class) and independent variables (physical and socioeconomic factors). The regression coefficients and AUC value for each LULC class are presented in Table 5. A positive (or negative) coefficient value indicates that the target LULC class was positively (or negatively) influenced by the factor. The primary determinant for waterbody transformation in the study area was elevation, with distance from roads ranking second in importance. Furthermore, elevation played a significant role in the conversion of all LULC classes, with different influencing values, while distance from roads was a crucial factor in the socioeconomic transition of all LULC classes.

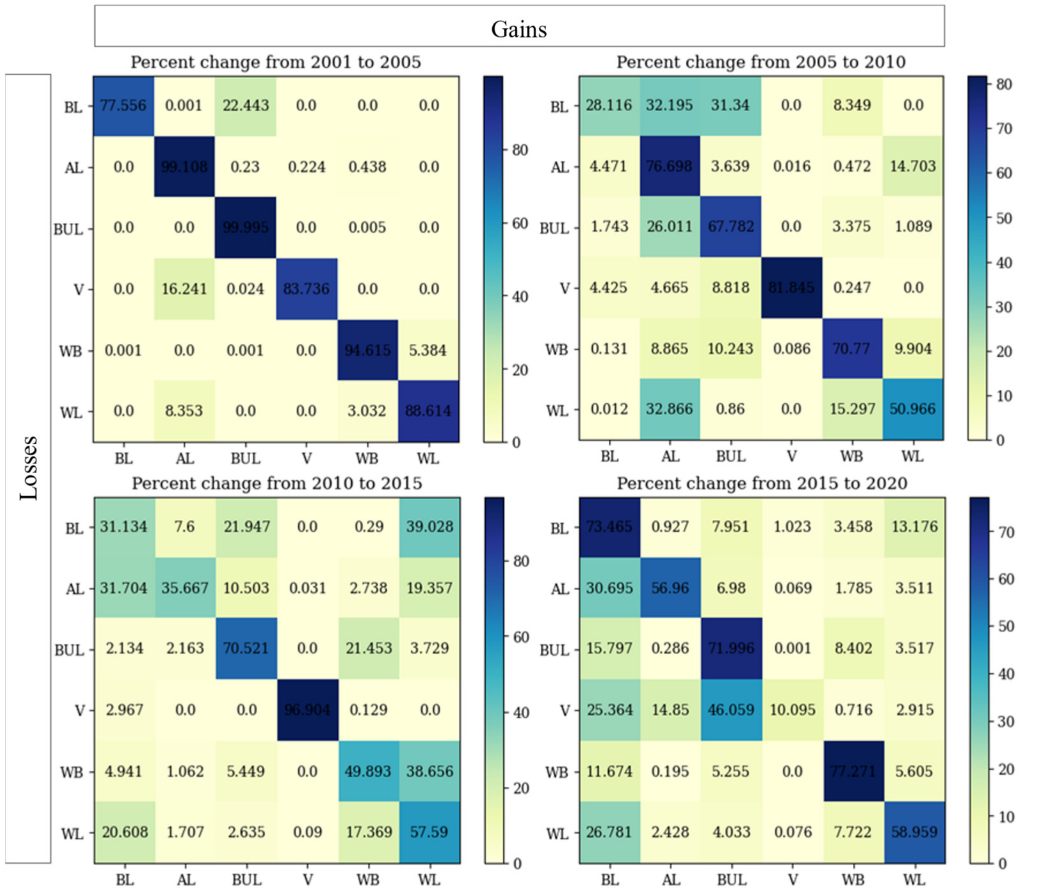

Figure 4. Percentage of conversion matrix for the inter-LULC class area changes from 2001 to 2020. BL= bare land, AL = agricultural land, BUL= built-up land, V = vegetation, WB = waterbody, WL = wetland.

Table 5. Results of the binary logistic regression model for the LULC class location preference as a function of physical and socioeconomic factors (2020).

Independent Variable	**Land Use Class (Dependent Variable)**					
	Bare Land	**Agricultural Land**	**Built-Up Land**	**Vegetation**	**Waterbody**	**Wetland**
Intercept	19.74	−26.77	−19.42	−24.83	5.60	10.04
Distance from commercial food services (m)	1.53×10^{-4} **	2.60×10^{-4} **	4.36×10^{-4} **	1.24×10^{-3} **	1.26×10^{-4} **	2.38×10^{-4} **
Distance from road (m)	-6.46×10^{-3} **	2.46×10^{-3} **	-1.10×10^{-2} **	-4.16×10^{-3} **	2.28×10^{-3} **	8.42×10^{-3} **
Elevation (m)	-1.46×10^{-1} **	1.80×10^{-1} **	1.38×10^{-1} **	1.47×10^{-1} **	-5.63×10^{-2} **	-9.21×10^{-2} **
Distance from streams (m)	-1.13×10^{-3} **	1.36×10^{-3} **	2.10×10^{-4} **	-3.05×10^{-3} **	3.08×10^{-4} **	1.16×10^{-3} **
Slope (degree)	-3.02×10^{-2} **	1.30×10^{-1} **	-1.50×10^{-2} *	2.00×10^{-2}	2.03×10^{-3}	-8.80×10^{-2} **
AUC	0.640	0.643	0.850	0.899	0.583	0.726

Note: N = 99,026 sample points; * p value < 0.05; ** p value < 0.001.

The above findings show that the decreases in agricultural and vegetation lands were associated with the expansion of built-up area or urbanization. Phompila et al. revealed that the increase in built-up area in Vientiane from 2016 to 2020 was due to the development of farmlands for residential, commercial, and economic purposes [29]. Since 2011, the special economic zone boundary located downstream of TLM has been introduced and started to develop [54], which attracted people who wanted to live and stay close to convenient facilities and new road networks. This development direction could therefore provide vital information for people selecting or developing their homes. According to Figure 3a–e, the expansion of bare land, waterbody, and wetland might be related to the replacement of land surfaces with soil and artificial lakes/ponds, which is consistent with previous studies in Vientiane by Faichia et al. and Vongpraseuth [30,55]. The increase in built-up area over TLM might result from unmanaged settlements due to the lack of enforcement of the land use plan. According to the Lao Statistic Bureau (2015) [37], the share of urban population in Laos increased from 27% to 33% during 2005–2015. The distance to roads significantly impacted all LULC classes, positively affecting waterbody, wetland, and agricultural land but negatively impacting vegetation, built-up land, and bare land. Settlements are commonly located near roads and bring about change in LULC classes due to the intensive human activity. This result is similar to cases in Aswan, Southern Egypt, and West Java Province, Indonesia [56,57].

TLM provides significant services in flood control and wastewater purification [58]. This marsh has a restricted range of biodiversity, containing only 41 species of vegetation that can be used for natural wastewater purification [31]. The continued growth of the special economic zone and residential zones might diminish biodiversity and compromise the effectiveness of the wetland's capacity for purification, leading to increased water pollution.

3.2. Water Quantity Estimation

As shown in Figure 5, the total water volume increased steadily at an average rate of 4129 m^3/year from 2001 to 2020. To further understand the details of the change, the distribution of water over TLM was identified in the northern, middle, and southern parts, as illustrated in Figure 6. During 2001–2020, the middle part exhibited a significant proportion of water volume. The northern part presented a rapid increase in water volume from 2982 to 11,020 m^3 between 2010 and 2020. This could be attributed to the new development of an artificial lake in the special economic zone [34,54]. The southern part fluctuated but slightly increased after 2010. Figure 6 illustrates the longitudinal profile of elevation and water surface where the marsh was developed from north to south. Clear changes were observed in the northern part from 2010 to 2015 and in the southern part from 2015 to 2020.

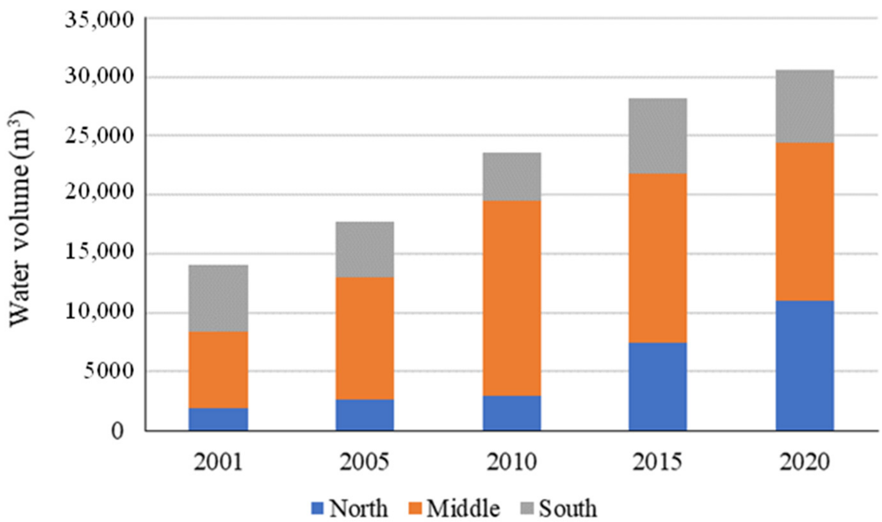

Figure 5. Distribution of water volume over TLM.

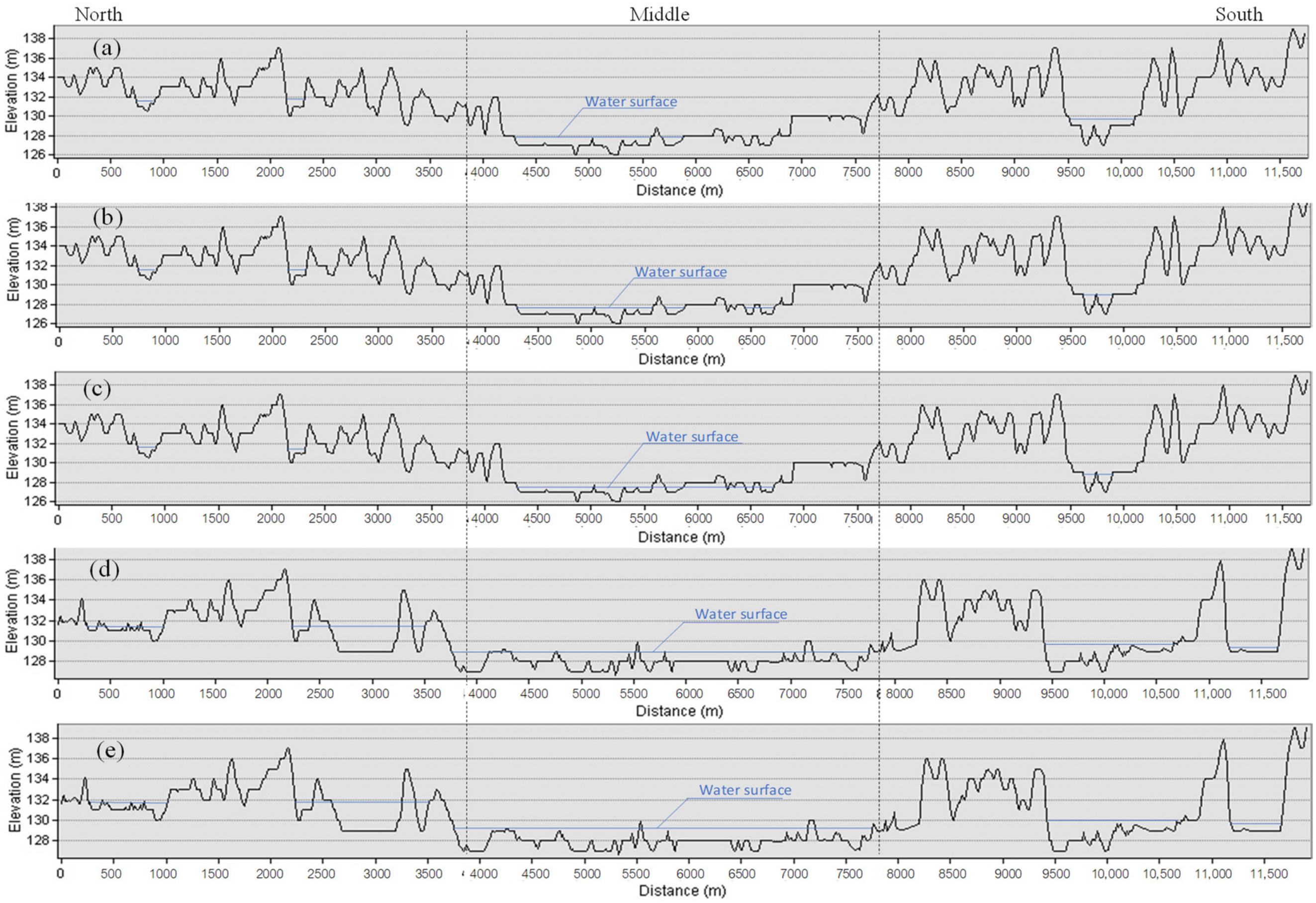

Figure 6. Elevation profile of TLM from north to south in (**a**) 2001, (**b**) 2005, (**c**) 2010, (**d**) 2015, and (**e**) 2020.

The correlation between changes in LULC area and water volume across different years was examined by nonparametric correlation analysis, as displayed in Figure 7. The built-up land, bare land, waterbody, and wetland exhibited a strongly positive relationship between area and water volume with Spearman's correlation coefficients (Rs) of 1.0, 1.0, 1.0, and 0.8, respectively. Conversely, agricultural and vegetation areas indicated strongly negative correlations of −0.9 and −1, respectively. The artificial lake and ponds occurred where the residential areas were located, and the land surface was developed before these water features were constructed. Therefore, built-up and bare land showed a strong relationship in changing the water volume. Additionally, built-up land, bare land, and waterbody were statistically significant ($p < 0.05$) in changing the water volume, whereas agricultural land and wetland were not statistically significant ($p \geq 0.1$). A case study in the Songkhram River Basin, Thailand, revealed that the development of a special economic zone was concurrent with an increase in streamflow from 5.30% to 6.35% [14], and a case in China revealed that an increase in construction and waterbody areas was linked to a loss of farmland [17]. These similar phenomena might be explained by the specific water resource conservation encouraged by the government of Lao PDR [54]. Such promotion could support a dilution effect, but the intensive discharge of pollutants due to expanded built-up areas is never negligible. Therefore, a comprehensive consideration of the multifaceted impacts of LULC change on the water environment is necessary for sustainable urban environmental planning.

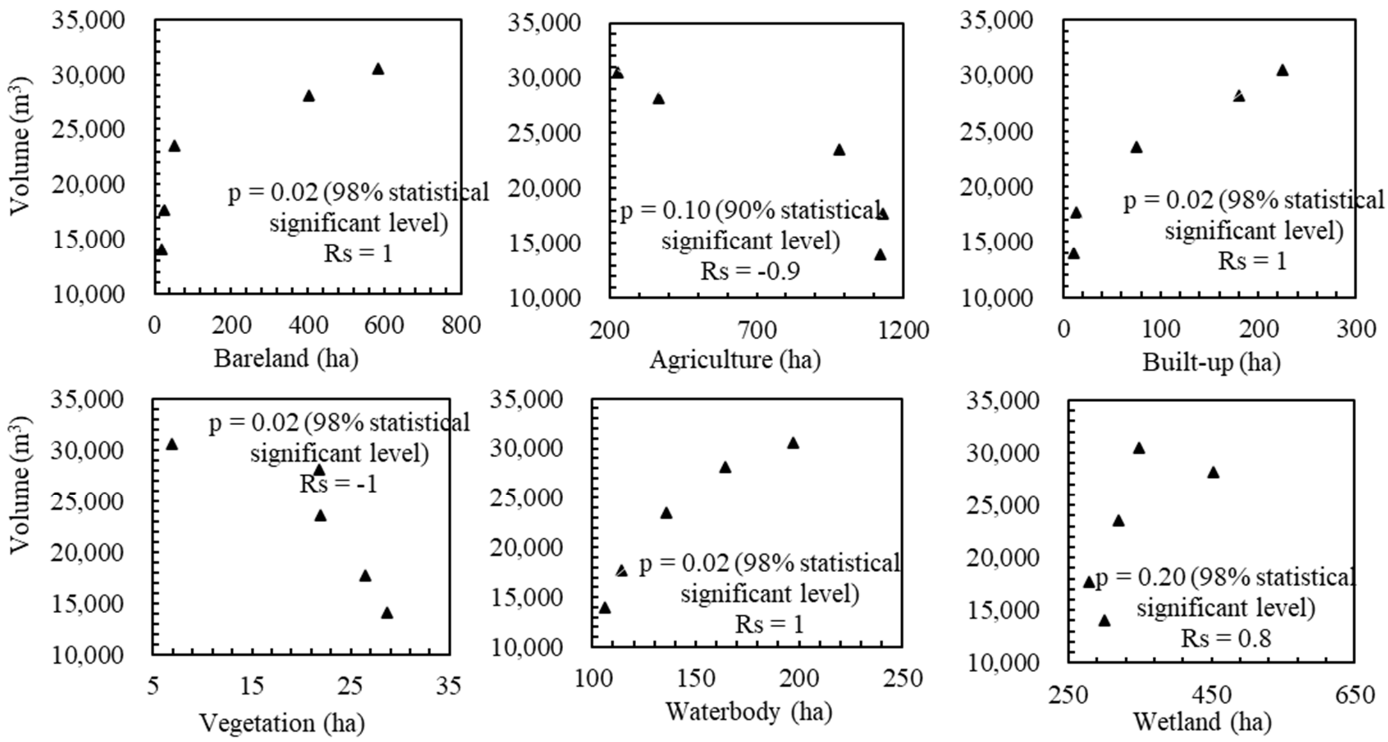

Figure 7. Correlation of water volume with land area of different LULC classes.

3.3. Nutrient Distribution

Nitrate-nitrogen export was evaluated in various scenarios for each LULC class, as illustrated in Table 6. The mean value indicates the average export scenario, while the minimum and maximum values correspond to the lowest and highest export scenarios, respectively. In terms of average exports, the wetland exhibited the highest level, followed by waterbody, built-up land, bare land, vegetation, and agricultural land. This may suggest the accumulation of nitrate-nitrogen rather than the self-production of nitrate-nitrogen in waterbody and wetland due to their lower elevations in the marsh. In contrast, the built-up area discharged a large amount of nitrate-nitrogen in three different scenarios compared to other LULC classes, which is similar to the results of Kulsoontornrat and Ongsomwang [49]. Furthermore, as illustrated in Figure 8, the northern region (especially the waterbody) exhibited a high load of nitrate-nitrogen, serving as the marsh outlet. Even though a high export was observed in the max scenario of all LULC classes, the min and mean scenarios were below 5 mg/L according to the Lao National Environmental Standard [59].

Table 6. Estimated nitrate-nitrogen export in different LULC classes in 2020.

LULC Class	LULC Area (ha) in 2020	NO_3^--N Export (kg/Year)			95% Confidence Interval of Mean	
		Min	Mean	Max	Lower	Upper
Bare land	583.09	577	8665	23,615	2966	14,622
Agricultural land	226.34	36	2261	6423	771	4009
Built-up land	224.28	6751	63,098	344,593	8314	148,268
Vegetation	6.94	0	3933	16,437	328	8039
Waterbody	197.24	6876	94,306	507,713	21,251	220,597
Wetland	349.30	6563	145,071	925,365	22,325	373,969
Sum	1587.19	20,803	317,334	1824,146	55,955	769,504

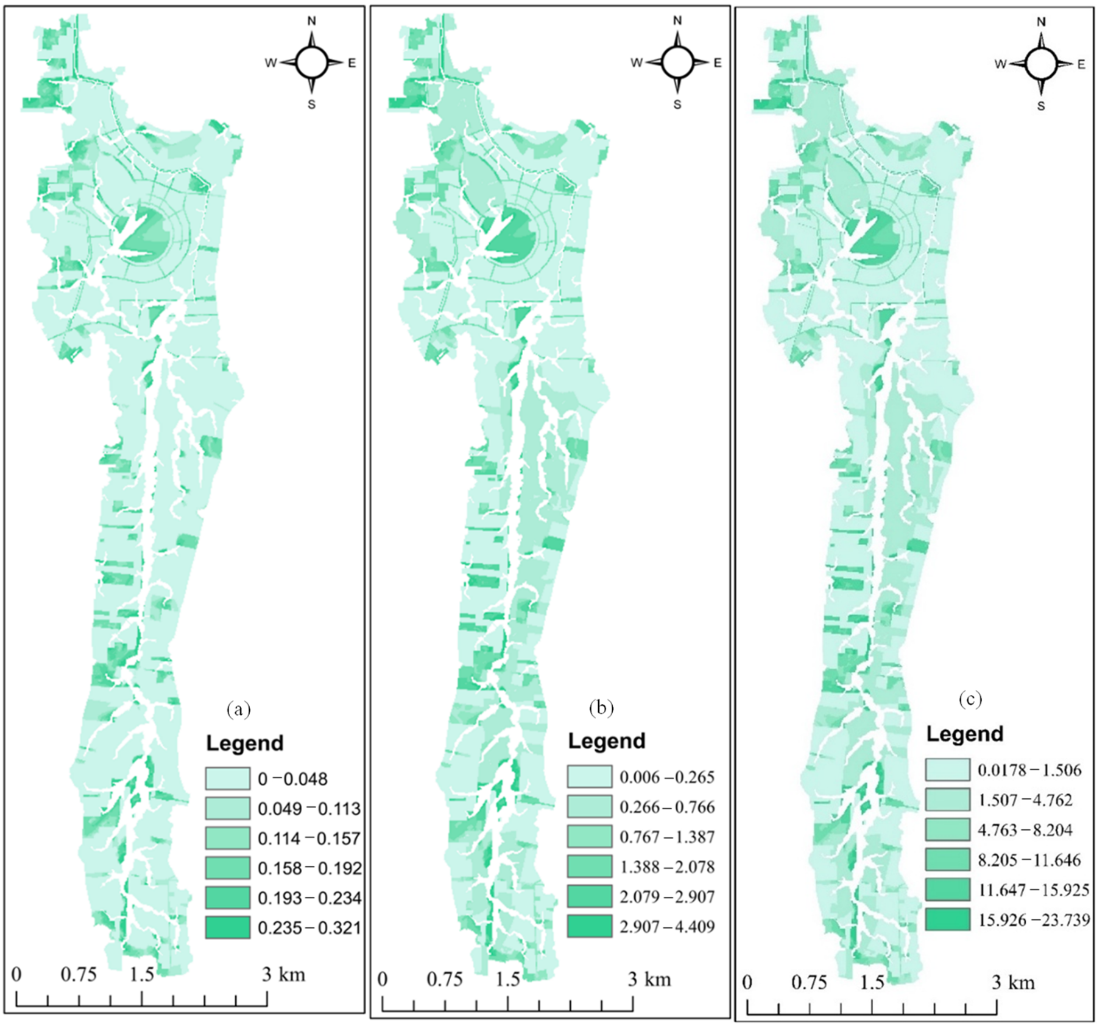

Figure 8. Distribution of nitrate-nitrogen load (kg/ha/year) in 2020 for the (**a**) minimum scenario, (**b**) mean scenario, and (**c**) maximum scenario.

The analysis of nitrate-nitrogen export using linear interpolation for each LULC class from 2010 to 2020 indicated increased levels in the wetland and waterbody over the years. This trend was similar to the proportion of nitrate-nitrogen export from built-up area, as shown in Figure 9a. This result might be related to the extent of the expansion of residential areas into the marsh, which may decrease the retention capability of natural surfaces. Changes in areas of LULC classes may impact the proportions of nitrate-nitrogen. In 2020, the total amount of nitrate-nitrogen was estimated to be 320,242 kg/year (estimated as bootstrap mean, slightly different from the actual mean). Similarly, Lei et al. and Permatasari et al. confirmed that the export of high total nitrogen concentrations is strongly related to the increase in urban land [9,20].

The vegetation presented the lowest land coverage ratio but the highest nitrate load compared to other LULC classes (see the sensitivity analysis in Figure 9b). It is possible that these outcomes resulted from the use of fertilizers in the fruit tree orchard, which were then carried into the watercourses through rainfall runoff. Conversely, even though bare land covered the largest area in 2020, it displayed a very low nitrate contribution, likely due to the absence of human activities. Case studies from other countries also found that high concentrations were accompanied by the excessive use of fertilizers in agricultural and built-up areas [23,25,28,60].

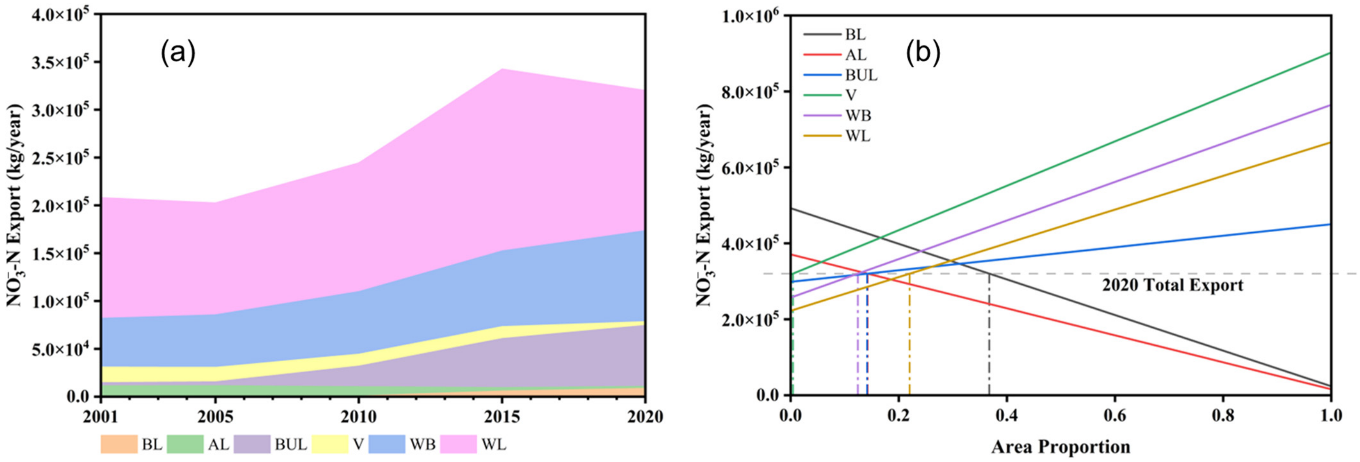

Figure 9. (**a**) Simulated total export of nitrate-nitrogen over time and (**b**) simulated variation in the total export of nitrate-nitrogen with the area proportions of different LULC classes.

As shown in Table 6, the high concentrations of pollutants produced by human activities in urban areas significantly affect water quality across seasons. Therefore, to ensure the sustainability of Vientiane's water environment, the critical solution is to enhance land use management by conserving urban wetland and waterbody areas and educating urban residents on controlling nitrate-nitrogen export. For instance, JICA conducted an experiment at a drainage canal leading to TLM and revealed that water spinach was capable of absorbing nitrogen and phosphorus at a rate of 0.1–0.2 mg/L/m^2 and <0.01 mg/L/m^2, respectively, per unit area covered [32]. Additionally, it was able to retain suspended solids of up to 0.19 kg/day/m^2 and reduce the flow velocity by 0.12–0.15 m/s. Therefore, TLM can be viewed as a nature-based solution for purifying domestic wastewater using various plant species, which presents a viable alternative approach for Vientiane. Simultaneously, it is crucial to enhance the responsibility of urban residents to become involved in pollutant control. These findings might be significant for the management of urban water environments in other similar developing countries, especially those experiencing rapid urbanization.

4. Conclusions

This study utilized Landsat images with the maximum likelihood method to classify the LULC of TLM in Vientiane, Laos. From 2001 to 2020, the bare land, built-up land, waterbody, and wetland areas increased by 29.92, 18.64, 0.87, and 0.16 times, respectively, whereas the agricultural and vegetation areas decreased by 0.80 and 0.76 times. Intensive exchange of waterbody with other LULC classes was witnessed over the years under the influence of physical and socioeconomic factors such as elevation and distance from roads. The total water volume increased from 14,036 m^3 in 2001 to 30,552 m^3 in 2020. The total nitrate-nitrogen export in 2020 reached 317 tons/year with a 95% confidence interval of (56, 770) tons/year, which would vary most sensitively with the vegetation land area according to the simulation. The findings could be attributed to the change in urban layout in TLM over the years: on the one hand, the road network expansion resulted in increased residential areas; on the other hand, an artificial lake increased the water volume for pollutant dilution. Therefore, it is necessary to develop comprehensive urban plans and prioritize related policies by emphasizing LULC management as a key factor in a sustainable urban water environment.

The Mekong River Basin is an important gateway for the China-proposed "Belt and Road Initiative", along which Thailand, Laos, Cambodia, Vietnam, Myanmar, and other countries have been developing more closely and rapidly since 2013. Within this region, TLM holds great significance as a highly representative area of the Mekong River Basin. The findings of the study can provide valuable references for managing urban water environments in other developing countries, particularly those situated along the Mekong

River in Southeast Asia, which are undergoing similar processes of urbanization. Moreover, this study may also have implications for the water environment protection, water resource utilization, and coordinated development of the Mekong River Basin.

Supplementary Materials: The following supporting information can be downloaded at https://www.mdpi.com/article/10.3390/w15244302/s1, Figure S1: Location of discrete monitoring points for different projects in the center of Vientiane Capital; Table S1: Satellite image and sources; Table S2: Confusion matrix results for LULC classification; Table S3: Flow rate at different monitoring points in Vientiane Capital; Table S4: Nutrient concentration monitored by JICA; Table S5: Nutrient load from Vientiane Capital at different monitoring points; Table S6: Calibration parameters for the NDR model.

Author Contributions: Conceptualization, K.X. and K.P.; methodology, K.X., K.P. and Y.L.; software, K.P. and Y.L.; validation, K.X. and Y.L.; formal analysis, K.P. and K.X.; investigation, K.P.; resources, K.P. and K.X.; data curation, K.P.; writing—original draft preparation, K.P.; writing—review and editing, K.X.; visualization, K.P. and Y.L.; supervision, K.X.; project administration, K.X.; funding acquisition, K.X. All authors have read and agreed to the published version of the manuscript.

Funding: This research was funded by the Fundamental Research Funds for the Central Universities (No. E2EG0502X2).

Data Availability Statement: Data are contained within the article and Supplementary Materials.

Acknowledgments: The authors would like to thank the Department of Environment of Laos and Space Eye Lao Sole Co., Ltd., for providing water quality and digital elevation model data. Dong Liu and Runkui Li of University of Chinese Academy of Sciences, Shuai Liang of Beijing Forestry University, and Tingwei Gao of Peking University are gratefully acknowledged for their insightful suggestions.

Conflicts of Interest: The authors declare no conflict of interest.

References

1. Oelsner, G.P.; Stets, E.G. Recent trends in nutrient and sediment loading to coastal areas of the conterminous U.S.: Insights and global context. *Sci. Total Environ.* **2019**, *654*, 1225–1240. [CrossRef]
2. Ross, E.R.; Randhir, T.O. Effects of climate and land use changes on water quantity and quality of coastal watersheds of Narragansett Bay. *Sci. Total Environ.* **2022**, *807*, 151082. [CrossRef]
3. Alikhani, S.; Nummi, P.; Ojala, A. Urban wetlands: A review on ecological and cultural values. *Water* **2021**, *13*, 3301. [CrossRef]
4. Almeida, C.M.R.; Sáez-Zamacona, I.; Silva, D.M.; Rodrigues, S.M.; Pereira, R.; Ramos, S. The role of estuarine wetlands (saltmarshes) in sediment microplastics retention. *Water* **2023**, *15*, 1382. [CrossRef]
5. EPA. Wetland Functions and Values. 2016. Available online: http://www.epa.gov/watertrain (accessed on 15 May 2023).
6. Ferreira, C.S.S.; Kašanin-Grubin, M.; Solomun, M.K.; Sushkova, S.; Minkina, T.; Zhao, W.; Kalantari, Z. Wetlands as nature-based solutions for water management in different environments. *Curr. Opin. Environ. Sci. Health* **2023**, *33*, 100476. [CrossRef]
7. Rimal, B.; Sharma, R.; Kunwar, R.; Keshtkar, H.; Stork, N.E.; Rijal, S.; Rahman, S.A.; Baral, H. Effects of land use and land cover change on ecosystem services in the Koshi River Basin, Eastern Nepal. *Ecosyst. Serv.* **2019**, *38*, 100963. [CrossRef]
8. Rotich, B.; Kindu, M.; Kipkulei, H.; Kibet, S.; Ojwang, D. Impact of land use/land cover changes on ecosystem service values in the cherangany hills water tower, Kenya. *Environ. Chall.* **2022**, *8*, 100576. [CrossRef]
9. Lei, C.; Wagner, P.D.; Fohrer, N. Influences of land use changes on the dynamics of water quantity and quality in the German lowland catchment of the Stör. *Hydrol. Earth Syst. Sci.* **2021**, *26*, 2561–2582. [CrossRef]
10. Mockler, E.M.; Shahumyan, H.; Williams, B.; Bruen, M. Loose one-way coupling of land use and nutrient emission models to assess effects of regional development scenarios on catchment water quality. *Environ. Model. Assess.* **2020**, *25*, 591–607. [CrossRef]
11. Xie, H.; Ringler, C. Agricultural nutrient loadings to the freshwater environment: The role of climate change and socioeconomic change. *Environ. Res. Lett.* **2017**, *12*, 104008. [CrossRef]
12. Lu, Y.; Song, S.; Wang, R.; Liu, Z.; Meng, J.; Sweetman, A.J.; Jenkins, A.; Ferrier, R.C.; Li, H.; Luo, W.; et al. Impacts of soil and water pollution on food safety and health risks in China. *Environ. Int.* **2015**, *77*, 5–15. [CrossRef] [PubMed]
13. Singh, H.; Singh, D.; Singh, S.K.; Shukla, D.N. Assessment of river water quality and ecological diversity through multivariate statistical techniques, and earth observation dataset of rivers Ghaghara and Gandak, India. *Int. J. River Basin Manag.* **2017**, *15*, 347–360. [CrossRef]
14. Shrestha, S.; Bhatta, B.; Shrestha, M.; Shrestha, P.K. Integrated assessment of the climate and landuse change impact on hydrology and water quality in the Songkhram River Basin, Thailand. *Sci. Total Environ.* **2018**, *643*, 1610–1622. [CrossRef] [PubMed]
15. Näschen, K.; Diekkrüger, B.; Evers, M.; Höllermann, B.; Steinbach, S.; Thonfeld, F. The impact of land use/Land cover change (LULCC) on water resources in a tropical catchment in Tanzania under different climate change scenarios. *Sustainability* **2019**, *11*, 7083. [CrossRef]

16. Gumindoga, W.; Rwasoka, D.; Ncube, N.; Kaseke, E.; Dube, T. Effect of landcover/land-use changes on water availability in and around Ruti dam in Nyazvidzi catchment, Zimbabwe. *Water SA* **2018**, *44*, 136–145. [CrossRef]
17. Liu, Y.; Long, H.; Li, T.; Tu, S. Land use transitions and their effects on water environment in Huang-huai-Hai plain, China. *Land Use Policy* **2015**, *47*, 293–301. [CrossRef]
18. Chaudhuri, A.S.; Singh, P.; Rai, S.C. Modelling LULC change dynamics and its impact on environment and water security: Geospatial technology based assessment. *Ecol. Environ. Conserv.* **2018**, *24*, S292–S298.
19. Elhag, M.; Psilovikos, A.; Sakellariou-Makrantonaki, M. Land use changes and its impacts on water resources in Nile delta region using remote sensing techniques. *Environ. Dev. Sustain.* **2013**, *15*, 1189–1204. [CrossRef]
20. Permatasari, P.A.; Setiawan, Y.; Khairiah, R.N.; Effendi, H. The effect of land use change on water quality: A case study in Ciliwung Watershed. *IOP Conf. Ser. Earth Environ. Sci.* **2017**, *54*, 012026. [CrossRef]
21. Hu, Y.; Zhang, K.; Li, Y.; Sun, Y.; Li, H.; Yang, G. Human activities increase the nitrogen in surface water on the eastern Loess Plateau. *Geofluids* **2021**, *2021*, 9957731. [CrossRef]
22. Chen, D.; Elhadj, A.; Xu, H.; Xu, X.; Qiao, Z. A study on the relationship between land use change and water quality of the Mitidja watershed in Algeria based on GIS and RS. *Sustainability* **2020**, *12*, 3510. [CrossRef]
23. Kändler, M.; Blechinger, K.; Seidler, C.; Pavlů, V.; Šanda, M.; Dostál, T.; Krása, J.; Vitvar, T.; Štich, M. Impact of land use on water quality in the upper Nisa catchment in the Czech Republic and in Germany. *Sci. Total Environ.* **2017**, *586*, 1316–1325. [CrossRef] [PubMed]
24. Camara, M.; Jamil, N.R.; Abdullah, A.F. Impact of land uses on water quality in Malaysia: A review. *Ecol. Process.* **2019**, *8*, 10. [CrossRef]
25. Cheng, C.; Zhang, F.; Shi, J.; Kung, H. What is the relationship between land use and surface water quality? A review and prospects from remote sensing perspective. *Environ. Sci. Pollut. Res.* **2022**, *29*, 56887–56907. [CrossRef] [PubMed]
26. Rodríguez-Romero, A.; Rico-Sánchez, A.; Mendoza-Martínez, E.; Gómez-Ruiz, A.; Sedeño-Díaz, J.; López-López, E. Impact of changes of land use on water quality, from tropical forest to anthropogenic occupation: A multivariate approach. *Water* **2018**, *10*, 1518. [CrossRef]
27. Bahar, M.M.; Ohmori, H.; Yamamuro, M. Relationship between river water quality and land use in a small river basin running through the urbanizing area of Central Japan. *Limnology* **2008**, *9*, 19–26. [CrossRef]
28. Xia, L.L.; Liu, R.Z.; Zao, Y.W. Correlation analysis of landscape pattern and water quality in Baiyangdian Watershed. *Procedia Environ. Sci.* **2012**, *13*, 2188–2196. [CrossRef]
29. Phompila, C.; Sihapanya, V.; Chanthavong, B.; Thongmanivong, S.; Van Khoa, P.; Noda, K.; Vadrevu, K.P. Agricultural land use/cover changes in the Vientiane, Laos. In *Remote Sensing of Agriculture and Land Cover/Land Use Changes in South and Southeast Asian Countries*; Springer: Chem, Switzerland, 2022; pp. 573–586. [CrossRef]
30. Faichia, C.; Tong, Z.; Zhang, J.; Liu, X.; Kazuva, E.; Ullah, K.; Al-Shaibah, B. Using RS data-based CA–Markov model for dynamic simulation of historical and future LUCC in Vientiane, Laos. *Sustainability* **2020**, *12*, 8410. [CrossRef]
31. Kyophilavong, P. *The Impact of Irrigation on Aquatic Wetland Resources: A Case Study of That Luang Marsh, Lao PDR*; Economy and Environment Program for Southeast Asia, IDRC Regional Office for Southeast and East Asia: Singapore, 2008.
32. JICA. *The Study on Improvement of Water Environment in Vientiane City Final Report*; JICA: Tokyo, Japan, 2011.
33. JICA. *The Project for Urban Water Environment Improvement in Vientiane Capital*; JICA: Tokyo, Japan, 2017.
34. Chanthavilay, M.; Wang, H.; Ying, W.; Li, F. Assessment of wastewater treatment in developing countries current practices in Vientiane Capital, LAOS. *Int. J. Adv. Res.* **2017**, *5*, 335–344. [CrossRef]
35. Claridge, C. *An Inventory of Wetlands of the Lao PDR*; Saeed, S., Ed.; IUCN: Gland, Switzerland, 1996.
36. Gerrard, P. *Integrating Wetland Ecosystem Values into Urban Planning: The Case of That Luang Marsh, Vientiane, Lao PDR*; IUCN — The World Conservation UnionAsia Regional Environmental Economics Programme and WWF Lao Country Office: Vientiane, Laos, 2004.
37. Lao Statistics Bureau. Population Census 2015. 2015. Available online: https://laosis.lsb.gov.la/ (accessed on 20 June 2023).
38. Rwanga, S.S.; Ndambuki, J.M. Accuracy assessment of land use/land cover classification using remote sensing and GIS. *Int. J. Geosci.* **2017**, *8*, 611–622. [CrossRef]
39. Seyam, M.M.H.; Haque, M.R.; Rahman, M.M. Identifying the land use land cover (LULC) changes using remote sensing and GIS approach: A case study at Bhaluka in Mymensingh, Bangladesh. *Case Stud. Chem. Environ. Eng.* **2023**, *7*, 100293. [CrossRef]
40. Wang, S.W.; Munkhnasan, L.; Lee, W.K. Land use and land cover change detection and prediction in Bhutan's high altitude city of Thimphu, using cellular automata and Markov chain. *Environ. Chall.* **2021**, *2*, 100017. [CrossRef]
41. Shiferaw, H.; Bewket, W.; Alamirew, T.; Zeleke, G.; Teketay, D.; Bekele, K.; Schaffner, U.; Eckert, S. Implications of land use/land cover dynamics and Prosopis invasion on ecosystem service values in Afar Region, Ethiopia. *Sci. Total Environ.* **2019**, *675*, 354–366. [CrossRef] [PubMed]
42. Gondwe, J.F.; Lin, S.; Munthali, R.M. Analysis of land use and land cover changes in urban areas using remote sensing: Case of Blantyre City. *Discret. Dyn. Nat. Soc.* **2021**, *2021*, 8011565. [CrossRef]
43. Mariye, M.; Jianhua, L.; Maryo, M. Land use and land cover change, and analysis of its drivers in Ojoje watershed, Southern Ethiopia. *Heliyon* **2022**, *8*, 09267. [CrossRef] [PubMed]
44. Islami, F.A.; Tarigan, S.D.; Wahjunie, E.D.; Dasanto, B.D. Accuracy assessment of land use change analysis using Google Earth in Sadar Watershed Mojokerto Regency. *IOP Conf. Ser. Earth Environ. Sci.* **2022**, *950*, 012091. [CrossRef]

45. Lemessa, D. A robust method of computing the annual rate of land use/land covers change in landscapes. *East Afr. J. Sci.* **2020**, *14*, 163–168.
46. Mandrekar, J.N. Receiver operating characteristic curve in diagnostic test assessment. *J. Thorac. Oncol.* **2010**, *5*, 1315–1316. [CrossRef]
47. Polo, T.C.F.; Miot, H.A. Use of roc curves in clinical and experimental studies. *J. Vasc. Bras.* **2020**, *19*, e20200186. [CrossRef]
48. Gil Pontius, R., Jr.; Schneider, L.C. Land-cover change model validation by an ROC method for the Ipswich watershed, Massachusetts, USA. *Agric. Ecosyst. Environ.* **2001**, *85*, 239–248. [CrossRef]
49. Kulsoontornrat, J.; Ongsomwang, S. Suitable land-use and land-cover allocation scenarios to minimize sediment and nutrient loads into kwan phayao, upper ing watershed, thailand. *Appl. Sci.* **2021**, *11*, 10430. [CrossRef]
50. Redhead, J.W.; May, L.; Oliver, T.H.; Hamel, P.; Sharp, R.; Bullock, J.M. National scale evaluation of the InVEST nutrient retention model in the United Kingdom. *Sci. Total Environ.* **2018**, *610–611*, 666–677. [CrossRef] [PubMed]
51. Benez-Secanho, F.J.; Dwivedi, P. Does Quantification of Ecosystem Services Depend Upon Scale (Resolution and Extent)? A Case Study Using the InVEST Nutrient Delivery Ratio Model in Georgia, United States. *Environments* **2019**, *6*, 52. [CrossRef]
52. Tikuye, B.G.; Gill, L.; Rusnak, M.; Manjunatha, B.R. Modelling the impacts of changing land use and climate on sediment and nutrient retention in Lake Tana Basin, Upper Blue Nile River Basin, Ethiopia. *Ecol. Model.* **2023**, *482*, 110383. [CrossRef]
53. Sharp, R.; Tallis, H.; Ricketts, T.; Guerry, A.; Wood, S.; ChaplinKramer, R.; Nelson, E.; Ennaanay, D.; Wolny, S.; Olwero, N.; et al. *InVEST 3.8.0 User's Guide*; Natural Capital Project: Stanford, CA, USA, 2020.
54. LTID (Lao ThatLuang Investment and Development). *Environmental Impact Assessment*; Lao ThatLuang Investment and Development (LTID): Vientiane, Laos, 2020.
55. Vongpraseuth, T. Reality of urbanization and urban master plan of Vientiane Capital, Lao PDR: Issues and prospects. *Am. Sci. J. Eng. Technol. Sci.* **2020**, *70*, 1–15.
56. Hamdy, O.; Zhao, S.; Salheen, M.A.; Eid, Y.Y. Analyses the driving forces for urban growth by using IDRISI®Selva models abouelreesh—Aswan as a case study. *Int. J. Eng. Technol.* **2017**, *9*, 226–232. [CrossRef]
57. Nahib, I.; Suryanta, J.; Niedyawati Kardono, P.; Turmudi Lestari, S.; Windiastuti, R. Integration of logistic regression and multicriteria land evaluation to simulation establishment of sustainable paddy field zone in Indramayu Regency, West Java Province, Indonesia. *IOP Conf. Ser. Earth Environ. Sci.* **2018**, *149*, 012005. [CrossRef]
58. MTPC; JICA. *The Survey on Existing Road and Drainage Conditions in Vientiane Municipality Project*; Ministry of Communication Transport Post and Construction, Department of Roads; Japan International Cooperation Agency: Vientiane, Laos, 2002.
59. Department of Pollution Control. *Decree on the Lao National Environmental Standard (No. 81)*; Ministry of Natural Resources and Environment: Vientiane, Laos, 2017.
60. Ahmad, W.; Iqbal, J.; Nasir, M.J.; Ahmad, B.; Khan, M.T.; Khan, S.N.; Adnan, S. Impact of land use/land cover changes on water quality and human health in district Peshawar Pakistan. *Sci. Rep.* **2021**, *11*, 16526. [CrossRef]